immunologic graft failure with cellular infiltration from endothelial graft failure, supported by the immunohistochemical detection of infiltrating CD4- and CD8-positive T cells in the case of immunologic failure only. Graft edema was classified as minimal, moderate, or severe, as described elsewhere.[18,21]

CEC Density of Preoperative and Postoperative Corneas

The CEC density was calculated for preoperative and postoperative mouse corneal grafts. To evaluate the effect of injecting 0.05% benzalkonium chloride into the anterior chamber, corneas were also observed immediately after treatment with benzalkonium. To count the CEC density of each cornea, the central region of the cornea was excised by using a 2-mm trephine and was placed on a glass slide with the endothelial side up. The posterior surface of the cornea was stained for 1 minute with 5% Alzarin red. The corneal tissue was inverted and covered with a coverglass, and the size and shape of the CECs were observed under an inverted light microscope (model BX-50; Olympus). Corneas seeded with fluorescein-labeled mouse CECs were observed for PKH26 fluorescence as whole mounts under a fluorescence microscope (models BH2-RFLT3 and BX50; Olympus). The number of cells in a 0.2 × 0.2-mm square was counted at 4 different sites on these corneas, and the average was calculated.

In Vivo and Cross-sectional Observation of Fluorescein-labeled CEC Attaching to Reconstituted Corneas

In the CEC allograft group, cells were observed on the day of surgery and at 1 and 4 weeks postoperatively under anesthesia by using a fluorescein microscope (models BH2-RFLT3 and BX50; Olympus). At 4 weeks after transplantation, 4 corneas were excised and embedded in optimal cutting temperature compound (Sakura Finetechnical, Tokyo, Japan) at −20°C. Frozen sections were cut at a thickness of 8 μm and placed on slides to observe fluorescein-labeled mouse CECs under the fluorescence microscope.

Histologic Examination After Transplantation

For histologic examination, 8 eyes per group were enucleated at 4 weeks after transplantation. Four eyes from each group were fixed in 10% formalin and processed by staining with hematoxylin–eosin for light microscopy. The other 4 eyes were fixed in 4% paraformaldehyde, frozen in optimal cutting temperature compound in acetone–dry ice and stored at −80°C. Frozen specimens were cut into 8-μm sections on a cryostat and dried in air. Approximately 15 sections were prepared from each group. Immunohistochemistry to detect CD4- and CD8-positive cells was performed by using these frozen sections from each group. Purified rat anti–mouse phycoerythrin-conjugated CD4 and fluorescein isothiocyanate–conjugated CD8 monoclonal antibodies (eBioscience, Tokyo, Japan) were used as the primary antibodies. After washing with PBS, sections were incubated with each primary antibody (diluted to 2.5 μg/mL) for 2 hours. After further washing with PBS, sections were stained with 4′, 6-diamidine-2′-phenylindole dihydrochloride (Roche Applied Science), mounted, and observed under fluorescein microscope (models BH2-RFLT3 or BX50; Olympus).

Statistical Analysis

The unpaired *t* test was used to compare mean values, as appropriate. All analyses were performed by using the Stat View statistical software package (Abacus Concepts, Berkeley, CA). The level of significance was set at $P < 0.05$ or $P < 0.01$.

RESULTS

Cell Density of Preoperative and Postoperative Corneas

The CEC density of normal corneas ranged from 1600 to 2500 cells/mm^2 (mean ± SD: 2038 ± 368 cells/mm^2; n = 4), and CECs showed a hexagonal morphology (Fig. 1A). No CECs were detected on the posterior surface of the cornea in the no endothelium group preoperatively, after endothelium had been removed with a cotton swab (Fig. 1B), on corneas immediately after treatment with 0.05% benzalkonium chloride (Fig. 1C), or on the peripheral cornea at 4 weeks after benzalkonium chloride treatment (Fig. 1D). These findings indicated that we could block the proliferation of CECs at the central and peripheral cornea during the observation period.

Fluorescein-labeled CECs with a hexagonal morphology were observed on the reconstituted corneas on day 0 (Figs. 1E,F) and at 4 weeks (Figs. 1G,H) after transplantation. Immediately after seeding with mouse cells, the CEC density of the reconstituted corneal grafts in the CEC allograft group ranged from 1250 to 2025 cells/mm^2 (mean, 1569 ± 336 cells/mm^2; n = 4). In postoperative week 4, the CEC density ranged from 1150 to 1600 cells/mm^2 (mean, 1400 ± 196 cells/mm^2; n = 4). Thus, the CEC density of the reconstituted corneas was maintained for 4 weeks, and no significant difference was detected between preoperative and postoperative corneas ($P > 0.05$).

A significant decrease of CECs was observed in the rejected grafts of the allograft group (Fig. 1I). The CEC density of rejected corneas ranged from 625 to 1125 cells/mm^2 (mean, 981 ± 239 cells/mm^2; n = 4). The cell density of rejected corneas in the allograft group was significantly lower than that of reconstituted corneas in the CEC allograft group ($P < 0.05$). These findings imply that the CEC layer is undoubtedly a target for effector cells during allograft rejection.

Clinical Findings After Corneal Transplantation

Up to week 4 postoperatively, the isograft group (n = 12) maintained corneal transparency in all cases. In contrast, transparency was not restored to any of the corneas from the no endothelium group (n = 13; Table 1). In the CEC allograft group (n = 12), eyes that showed the disappearance of fluorescein-tagged cells within 4 weeks after surgery (n = 3) were defined as having endothelial graft failure, because no CD4- or CD8-positive infiltrating cells were detected in the host or graft tissues immunohistochemically. The graft

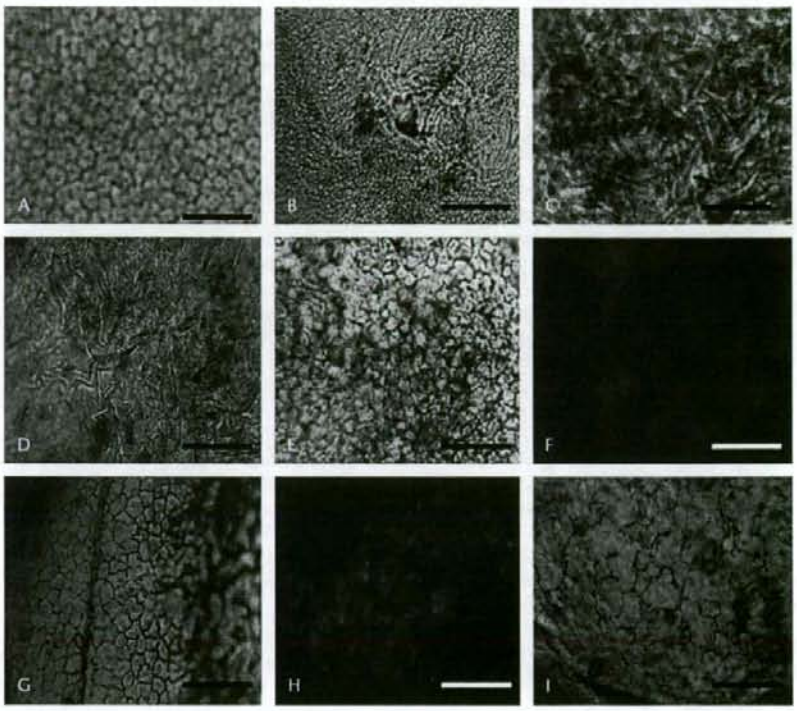

FIGURE 1. Representative findings of the endothelium in preoperative and postoperative corneas. A, Typical hexagonal morphology of CECs in a normal control cornea is shown by Alzarin red S staining. B, No staining is observed in a cornea denuded of endothelium by scraping with a cotton swab. C, Treatment with 0.05% benzalkonium chloride also removed CECs, as shown by no Alzarin red S staining of the posterior corneal surface. D, At the periphery of a cornea from the no endothelium group, CECs are not observed at 4 weeks after injury with 0.05% benzalkonium chloride. E, Preoperative Alzarin red S staining of a reconstituted cornea shows hexagonal cells after CECs were seeded onto a cornea denuded of endothelium in the CEC allograft group. F, CECs are totally PKH26-GL positive under a fluorescence microscope. G, Hexagonal cells are observed by Alzarin red S staining of a reconstituted cornea at 4 weeks after transplantation in the CEC allograft group. H, On fluorescence microscopy of the same cornea as shown in G, CECs are all PKH26-GL positive (red). I, Alzarin red S staining of rejected CECs in the allograft group shows an increase of cell size and decrease of density. Bars = 100 μm.

survival rate was 100% in the isograft group (n = 12), 0% in the no endothelium group (n = 13), 33% in the allograft group (n = 18), and 75% in the CEC allograft group (n = 12). The graft survival rate was significantly higher in the CEC allograft group than in the allograft group ($P < 0.05$; Table 1). Representative anterior-segment photographs from each group at 4 weeks after transplantation are shown in Figures 2A–D. A total of 67% of the corneal grafts in the allograft group and 100% of grafts in the no endothelium group showed corneal edema and opacity (Figs. 2B,C). In the CEC allograft group, fluorescence microscopy demonstrated that fluorescein-labelled CECs were present in the graft site at 4 weeks after transplantation in 9 corneas per 12 operated eyes (Fig. 2E).

TABLE 1. Rejection Rate and Endothelial Graft Failure Rate at 4 Weeks After Transplantation

Group	Graft Survival Rate (%)	Rejection Rate (%)	Endothelial Graft Failure Rate (%)
Isograft	12/12 (100)	0/12 (0)	0/12 (0)
No endothelium	0/13 (0)	0/13 (0)	13/13 (100)
Allograft	6/18 (33)	12/18 (67)	0/18 (0)
CEC allograft	9/12 (75)	0/12 (0)	3/12 (25)

The incidence of graft failure was significantly lower in the CEC allograft group than that in the allograft group. The graft survival rate was 100% in the isograft group, 0% in the no endothelium group, 33% in the allograft group, and 75% in the CEC allograft group. The graft survival rate was significantly higher in the CEC allograft group than in the allograft group ($P < 0.05$).

Histologic and Immunohistochemical Findings at 4 Weeks After Transplantation

In the isograft group, there was no edema and no infiltrating cells at 4 weeks after transplantation. The corneal endothelial layer was intact (Fig. 3A). Proliferation of CECs on the Descemet membrane was not detected in the no endothelium group (Fig. 3B). The grafts showed severe edema and few infiltrating cells, whereas the Descemet membrane was severely damaged (broken black arrows). In the allograft group, the corneal grafts showed many infiltrating cells, which caused opacity of the grafts (Fig. 3C). Immunohistochemistry revealed many CD4- and CD8-positive cells infiltrating into the transplanted allografts, suggesting the occurrence of immunologic rejection (Fig. 3D). In the CEC allograft group, neither infiltrating cells nor stromal edema was observed (Fig. 3E). CECs were detected on the Descemet membrane of the reconstituted corneas and formed a monolayer at 4 weeks after transplantation. These cells were PKH26 positive by fluorescence microscopy, indicating that they were transplanted mouse CECs and not host-derived CECs (Fig. 3F, black

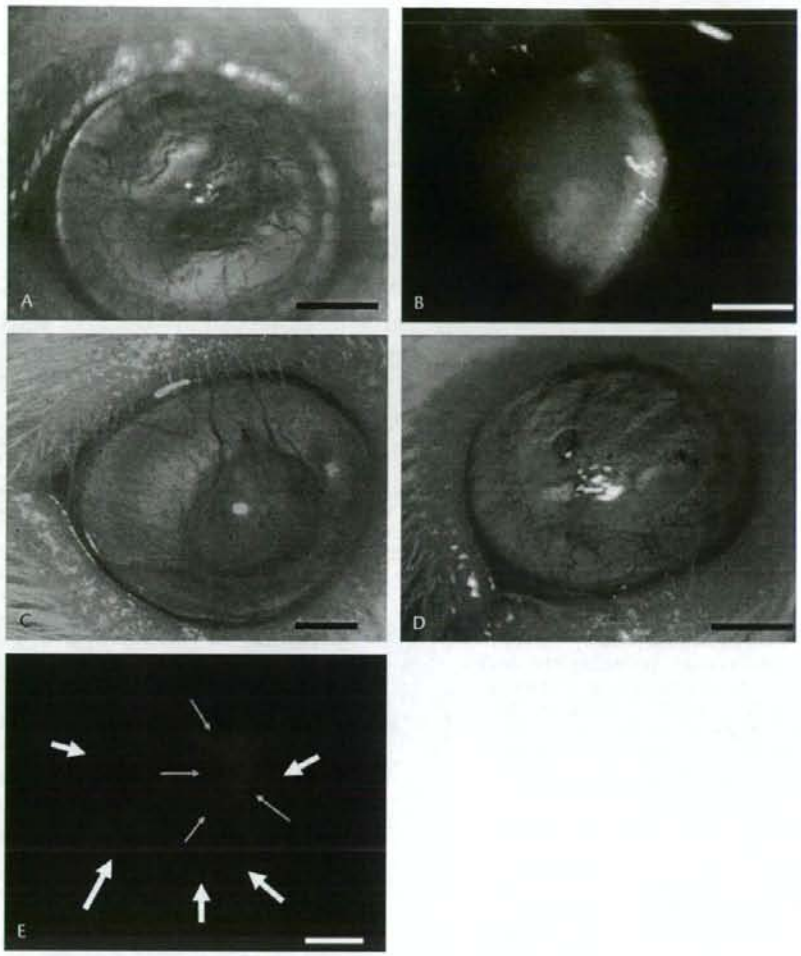

FIGURE 2. Anterior-segment photographs from the 4 groups. Representative anterior-segment photographs were obtained at 4 weeks after transplantation by using an operating microscope, a slit-lamp microscope, and a fluorescein microscope. A, In the isograft group, the corneal graft is transparent without opacity, edema, or neovascularization. B, In the no endothelium group, the corneal graft shows severe edema by slit-lamp microscopy. C, In the allograft group, there is severe corneal opacity with moderate neovascularization and edema. D, In the CEC allograft group, the graft is transparent at 4 weeks after transplantation. E, fluorescein-labeled CECs are clearly detected, and most of the graft is covered with transplanted CECs (green and white arrows show the margin of the graft and eye, respectively; bars = 1 mm).

arrows). Immunohistochemical analysis showed no infiltration of CD4- or CD8-positive T cells (Fig. 3G).

DISCUSSION

Joo et al[22] introduced a mouse CEC transplantation model and showed that cultured CECs are functional in vivo. We modified their model to make an appropriate system for immunologic analysis of CEC allograft procedures by using cultured allo-CECs and transplantation onto corneas with endothelial deficiency. In all of the mouse corneal transplantation models described elsewhere, the graft bed was normal cornea,[21,23] so these models are similar to the situation of transplantation for keratoconus and corneal stromal dystrophy in humans. Therefore, we developed a mouse bullous keratopathy model to reproduce the clinical setting of human bullous keratopathy. As summarized in Table 1, we found that corneal transparency was maintained in the full-thickness syngeneic transplantation model (isograft group), whereas corneal grafts never recovered transparency during the observation period in the no endothelium group. These findings suggest the validity of our experimental model. In this study, we also performed histologic examination and evaluated the occurrence of allograft rejection to distinguish immunologic graft failure from endothelial failure. In contrast to the rejection rate of 67% in the allograft group, there was no immunologic rejection (including histologic evidence) in the CEC allograft group (Table 1). These data strongly suggest that the outcome of allogeneic CEC transplantation is better than that of allogeneic full-thickness corneal transplantation from the standpoint of the immune response, although further long-term observation is needed.

In the CEC allograft group, there was no evidence of an inflammatory reaction, such as massive cellular infiltration, keratic precipitates, or fibrin deposition, in the anterior chamber under slit-lamp microscopy, providing further

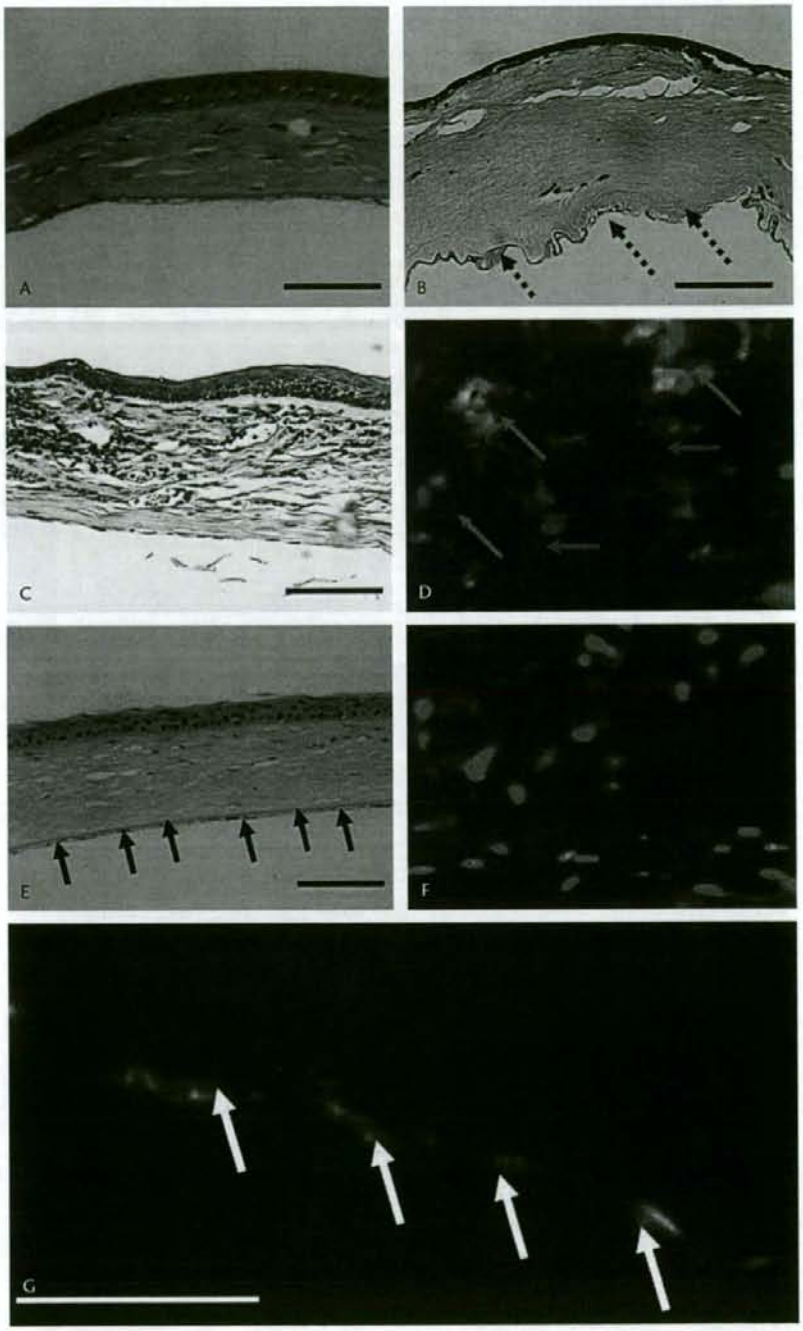

FIGURE 3. Histologic and immunohistochemical findings at 4 weeks after transplantation. A, There is no corneal stromal edema and no infiltrating cells in the isograft group. B, In the no endothelium group, the corneal graft shows severe edema and few infiltrating cells. The Descemet membrane is injured (broken black arrows). C, Many mononuclear cells are infiltrating the graft from the allograft group. The immunologic reaction induced by these infiltrating cells probably caused the clinically identified stromal opacity. D, In the allograft group, immunohistochemical study shows many infiltrating CD4-positive (red cells, pink arrows) and CD8-positive cells (green cells, green arrows) in the graft. Nuclei are stained with DAPI (blue). E, Neither infiltrating cells nor stromal edema can be observed in the CEC allograft group. Transplanted CECs are detected on the Descemet membrane of reconstituted corneas and form a monolayer at 4 weeks after transplantation (black arrows). F, In the CEC allograft group, no $CD4^{-}$-positive (red) or $CD8^{-}$-positive (green) cells are detected in the corneal graft. Nuclei are stained with DAPI (blue). G, Monolayer of transplanted CECs stained with PKH-26 on the Descemet membrane of a reconstituted cornea under fluorescein microscopy [white arrows; bars = 100 μm; original magnification = ×40 (A, B, C, E), ×200 (D, F), and ×100× (G)].

evidence that there was no notable immunologic rejection. The lack of CD4- or CD8-positive cells in the CEC allograft group also supported the absence of an immune reaction in edematous grafts with endothelial failure or clear grafts without edema (data not shown). However, the exact mechanism of immunologic escape in the CEC allograft group is unknown. A possible mechanism may be related to the character of the Descemet membrane, which blocks the

passage of antigen-presenting cells such as dendritic cells. As a consequence, antigen-presenting cells only travel through the aqueous humor and cannot efficiently present allo-antigens to host T cells. Moreover, we cannot deny the possibility that our short follow-up period with a low antigen load did not elicit enough sensitization to cause discernible acute allograft rejection. Further analysis of why allo-CEC transplantation has immune advantages over full-thickness corneal transplantation is ongoing at our laboratory.

It is important to address the drawbacks of this study. Apart from cell or sheet transplantation of cultured CECs with the goal of clinical application, full-thickness trephination is done in the mouse CEC allograft model, but this technique is not completely consistent with the ideal for CEC transplantation. However, despite the highly invasive operation performed in this study, the rejection rate was remarkably low. This finding suggests that cell or sheet transplantation without trephination may have further advantages in CEC allotransplantation. The occurrence of graft edema and endothelial failure without rejection may imply the limited survival of cultured CECs in the CEC allograft group. Moreover, the observation period was only 4 weeks in this study. We should accumulate immunologic data over an extended observation period, considering the maximum duration of graft edema in the no endothelium group.

In summary, we created a mouse model of bullous keratopathy and compared the clinical course of CEC allografts with that of full-thickness conventional allografts. Our findings strongly suggest that the outcome of allogeneic CEC transplantation is better than that of allogeneic full-thickness corneal transplantation from the standpoint of the immune response. Our CEC allograft model for bullous keratopathy may be useful for the study of corneal transplantation, regenerative medicine, and immunology.

ACKNOWLEDGMENTS

The authors appreciate critical comments of Junji Hamuro and Jun Yamada and miscellaneous support of Hiroe Morita and Shin Hato.

REFERENCES

1. Terry MA, Ousley PJ. Replacing the endothelium without corneal surface incisions or sutures: the first United States clinical series using the deep lamellar endothelial keratoplasty procedure. *Ophthalmology.* 2003;110: 755–764.
2. Borboli S, Colby K. Mechanisms of disease: Fuch's endothelial dystrophy. *Ophthalmol Clin North Am.* 2002;15:17–25.
3. Stechschulte SU, Azar DT. Complications after penetrating keratoplasty. *Int Ophthalmol Clin.* 2000;40:27–43.
4. Ko W, Freuh B, Shield C, et al. Experimental posterior lamellar transplantation of the rabbit cornea. *Invest Ophthalmol Vis Sci.* 1993;34: S1102.
5. Melles GR, Eggink FA, Lander F, et al. A surgical technique for posterior lamellar keratoplasty. *Cornea.* 1998;17:618–626.
6. Terry MA. The evolution of lamellar grafting techniques over twenty-five years. *Cornea.* 2000;19:611–616.
7. Terry MA, Ousley PJ. Deep lamellar endothelial keratoplasty visual acuity, astigmatism, and endothelial survival in a large prospective series. *Ophthalmology.* 2005;112:1541–1548.
8. Melles GR, Lander F, van Dooren BT, et al. Preliminary clinical results of posterior lamellar keratoplasty through a sclerocorneal pocket incision. *Ophthalmology.* 2000;107:1850–1856.
9. Gorovoy MS. Descemet-stripping automated endothelial keratoplasty. *Cornea.* 2006;25:886–889.
10. Mimura T, Shimomura N, Usui T, et al. Magnetic attraction of iron-endocytosed corneal endothelial cells to Descemet's membrane. *Exp Eye Res.* 2003;76:745–751.
11. Mimura T, Yamagami S, Usui T, et al. Long-term outcome of iron-endocytosing cultured corneal endothelial cell transplantation with magnetic attraction. *Exp Eye Res.* 2005;80:149–157.
12. Mimura T, Yamagami S, Yokoo S, et al. Sphere therapy for corneal endothelium deficiency in a rabbit model. *Invest Ophthalmol Vis Sci.* 2005;46:3128–3135.
13. Mimura T, Yokoo S, Araie M, et al. Treatment of rabbit bullous keratopathy with precursors derived from cultured human corneal endothelium. *Invest Ophthalmol Vis Sci.* 2005;46:3637–3644.
14. Mimura T, Yamagami S, Yokoo S, et al. Cultured human corneal endothelial cell transplantation with a collagen sheet in a rabbit model. *Invest Ophthalmol Vis Sci.* 2004;45:2992–2997.
15. Hsiue GH, Lai JY, Chen KH, et al. A novel strategy for corneal endothelial reconstruction with a bioengineered cell sheet. *Transplantation.* 2006;81: 473–476.
16. Yue BYJT, Sugar J, Gilboy JE, et al. Growth of human corneal endothelial cells in culture. *Invest Ophthalmol Vis Sci.* 1989;30:248–253.
17. Joo CK, Pepose JS, Fleming TP. In vitro propagation of primary and extended life span murine corneal endothelial cells. *Invest Ophthalmol Vis Sci.* 1994;35:3952–3957.
18. Niederkorn JY, Mellon J. Anterior chamber-associated immune deviation promotes corneal allograft survival. *Invest Ophthalmol Vis Sci.* 1996;37: 2700–2707.
19. Jumblatt MM, Maurice DM, McCulley JP. Transplantation of tissue-cultured corneal endothelium. *Invest Ophthalmol Vis Sci.* 1978;17:1135–1141.
20. Yang HJ, Sato T, Matsubara M, et al. Endothelial wound-healing in penetrating corneal graft for experimental bullous keratopathy in rabbit. *Jpn J Ophthalmol.* 1985;29:378–393.
21. Sonoda Y, Streilein JW. Impaired cell-mediated immunity in mice bearing healthy orthotopic corneal allografts. *J Immunol.* 1993;150:1727–1734.
22. Joo CK, Green WR, Pepose JS, et al. Repopulation of denuded murine Descemet's membrane with life-extended murine corneal endothelial cells as a model for corneal cell transplantation. *Graefes Arch Clin Exp Ophthalmol.* 2000;238:174–180.
23. Yamagami S, Dana MR, Tsuru T. Draining lymph nodes play an essential role in alloimmunity generated in response to high-risk corneal transplantation. *Cornea.* 2002;21:405–409.

Tissue Antigens ISSN 0001-2815

BRIEF COMMUNICATION

Mutation screening of the *CARD15* gene in sarcoidosis

M. Akahoshi[1,2,3], M. Ishihara[4,5], K. Namba[6], N. Kitaichi[6], Y. Ando[7], S. Takenaka[8], T. Ishida[5], S. Ohno[6], N. Mizuki[4], H. Nakashima[2,9] & T. Shirakawa[1]

1 Laboratory for Genetics of Allergic Diseases, SNP Research Center, The Institute of Physical and Chemical Research (RIKEN), Yokohama, Japan
2 Department of Medicine and Biosystemic Science, Graduate School of Medical Sciences, Kyushu University, Fukuoka, Japan
3 Department of Internal Medicine, Chihaya Hospital, Fukuoka, Japan
4 Department of Ophthalmology and Visual Science, Yokohama City University School of Medicine, Yokohama, Japan
5 Hiyoshi Eye Clinic, Yokohama, Japan
6 Department of Ophthalmology and Visual Sciences, Hokkaido University Graduate School of Medicine, Sapporo, Japan
7 Department of Ophthalmology, Keio University School of Medicine, Tokyo, Japan
8 Department of Respiratory Diseases, Kumamoto City Hospital, Kumamoto, Japan
9 Division of Nephrology and Rheumatology, Department of Internal Medicine, Fukuoka University School of Medicine, Fukuoka, Japan

Key words
Blau syndrome; CARD15; Crohn's disease; early-onset sarcoidosis; mutation; sarcoidosis

Correspondence
Mitsuteru Akahoshi, MD, PhD
Department of Internal Medicine
Chihaya Hospital
2-30-1 Chihaya
Higashi-ku
Fukuoka 813-8501
Japan
Tel: +81 92 661 2211
Fax: +81 92 683 0411
e-mail: akahoshi@intmed1.med.kyushu-u.ac.jp

Received 1 January 2008; revised 19 February 2008; accepted 11 March 2008

doi: 10.1111/j.1399-0039.2008.01043.x

Abstract

CARD15 was first identified as a susceptibility gene for Crohn's disease. More recently, *CARD15* mutations were shown to be associated with the pediatric granulomatous inflammatory diseases, Blau syndrome and early-onset sarcoidosis (EOS). The aim of the present study was to evaluate whether *CARD15* variants also play a role in patients with ordinary sarcoidosis other than EOS. We enrolled 135 Japanese sarcoidosis patients with uveitis as well as 95 healthy individuals and performed mutation analysis by direct sequencing of *CARD15* exon 4. Direct DNA sequencing in the sarcoidosis patients showed eight *CARD15* variants, including five novel mutations (13402C>T, 13543C>T, 13775C>A, 13937G>A, and 14079C>T). Compared with healthy individuals, *CARD15* mutations are not common in the Japanese patients with sarcoidosis. Based on the results, we examined the clinical manifestations in patients with sarcoidosis according to their *CARD15* mutations. Sarcoidosis patients with these mutations have no specific clinical features with regard to course of the disease or disease severity. Our results indicate that in general, *CARD15* mutations may not contribute to the risk of sarcoidosis.

Sarcoidosis is a chronic systemic disorder of unknown etiology characterized by the formation of noncaseating granuloma in affected organs, particularly the lung (1). Although the cause of sarcoidosis is still unclear, exposure to specific transmissible environmental agents has been implicated in the etiology of this disease. Moreover, racial differences in disease incidence or severity as well as familial clustering of cases strongly support the role of genetic susceptibility to sarcoidosis. To date, several candidate genes have been proposed to play a role in sarcoidosis. We have recently showed an association between the *IFNA* genotype and the risk of sarcoidosis (2). Moreover, the human leukocyte antigen class II allele and single nucleotide polymorphisms (SNPs) in the *BTNL2* gene have recently been associated with sarcoidosis susceptibility in different populations (3–5).

Two distinct forms of sarcoidosis exist in children. Older children usually present with a multisystemic disease similar to the adult manifestation, with frequent hilar lymphadenopathy and lung involvement. In contrast, early-onset sarcoidosis (EOS), which usually manifests before 4 years, is quite rare and has a unique manifestation of the disease characterized by a distinct triad of skin rash, uveitis, and arthritis (6). Blau syndrome (BS) is an autosomal dominant disease characterized by the early childhood onset of granulomatous inflammatory arthritis, uveitis, and skin rash. The genetic locus linked to BS was mapped to the chromosomal region 16q12-q21 (7) and then found to be

associated with mutations in the *CARD15* gene (8). EOS is clinically indistinguishable from BS, except lacking a clear dominant inheritance pattern (family history) of the disease. Recent genetic analysis in 10 Japanese patients with EOS showed that most of the patients had heterozygous missense mutations in *CARD15*, which suggests that EOS and BS have common genetic etiologies (9).

Similar to BS and EOS, known disease-associated *CARD15* mutations result in a dramatic clinical phenotype in early childhood, while more subtle variations in the *CARD15* gene that result in only partial functional alteration of the protein may play a role in the susceptibility to sarcoidosis. Therefore, we hypothesized that some *CARD15* variants may be associated with ordinary (adult type) sarcoidosis in similar manner to which they are with EOS. To test this hypothesis and to further assess the role of *CARD15* in granulomatous inflammatory disease, we performed mutation analysis by direct sequencing of *CARD15* in Japanese patients with sarcoidosis and compared the result with healthy controls. Because the mutations observed in EOS and BS are located within or near the central nucleotide-binding domain (NBD), we focused on *CARD15* exon 4 that covers the entire NBD and determined the nucleotide sequence. We excluded analysis regarding three major *CARD15* variants (R702W, G908R, and 1007fs) associated with Crohn's disease (CD) because of lack of common CD-associated variants in the Japanese population (10, 11).

We enrolled 135 Japanese patients with sarcoidosis (mean age 46.8 years; range 10–78 years; 101 women and 34 men) who were recruited between 1989 and 1993 mainly from the Department of Ophthalmology at Yokohama City University School of Medicine and Japanese Red Cross Medical Center. Sarcoidosis was diagnosed on the basis of the radiographic and clinical presentation including uveitis, and the finding of noncaseating granulomas in biopsy specimens with negative special stains and cultures for acid-fast bacilli and fungi. The controls were 95 randomly selected healthy individuals (mean age 35.4 years; range 20–44 years; 65 females and 30 males) who had no history of pulmonary disease or other inflammatory diseases, including CD. All subjects in this study were of Japanese ethnicity and gave their written informed consent for participation in the study, according to the process approved by the ethics committee at the SNP Research Center, Institute of Physical and Chemical Research.

To identify variants in the *CARD15* gene, we sequenced exon 4 of *CARD15* along with its neighboring introns in 135 patients with sarcoidosis from our study cohort. As controls, we further sequenced *CARD15* exon 4 in 95 healthy individuals. Overlapping polymerase chain reaction (PCR) products were generated using three primer pairs: 5′-ATTGTCTGGTTAGGTCCCGT-3′ and 5′-TTGAACTCGGTGCGGATGTA-3′, 5′-AGTTCAGGTTCACGGATCGT-3′ and 5′-TGGCCTGCCACAATTGAAGA-3′, and 5′-CCTGGAATTCCTTCACATCAC-3′ and 5′-CACTTAGCCTTGATGGTGCT-3′. For each PCR, 5 ng of genomic DNA was amplified in a total reaction volume of 10 μl containing 12.5 pmol of each primer, 3.9 mM $MgCl_2$, 1.25 mM of each dNTP, 0.5 U *Taq* polymerase. The cycling conditions were an initial denaturation at 95°C for 2 min, followed by 37 cycles at 94°C for 30 s, 60°C for 30 s, and 72°C for 3 min, with a final extension at 72°C for 7 min. Each fragment amplified by PCR was sequenced using the BigDye Terminator (Applied Biosystems, Foster City, CA) on an ABI Prism 3700 Genetic Analyzer (Applied Biosystems). The sequences were analyzed and variants were identified using the SEQUENCHER program (Gene Codes Corporation, Ann Arbor, MI). Genomic DNA samples were extracted from whole peripheral blood by using standard protocols.

Direct DNA sequencing of the indicated region, including exon 4, in 135 patients with sarcoidosis showed eight *CARD15* variants: 13402C>T (T245I), 13543C>T (A292V), 13599C>T (R311W), 13775C>A (D369E), 13937G>A (V423V), 14079C>T (R471C), 14429T>G (R587R), and 14502G>A (A612T) (Table 1). The distributions of all variants were in Hardy–Weinberg equilibrium in both the sarcoidosis and control groups. Nucleotide position 1 (+1) was defined as the first adenine of the initiation codon (ATG), and the positions of the SNPs were described relative to the initiation codon. Among the eight variants, two are synonymous substitutions and the other six are missense mutations. The missense mutations R311W and A612T, which were found in cases 3 and 11, respectively, have been reported previously in European patients with inflammatory bowel disease (IBD) (12). In addition, the A612T mutation has also been reported recently in Japanese patients with EOS but appears to have no association with EOS (9). Thus, no EOS/BS-related mutations were detected in our sarcoidosis patients. The synonymous 14429T>G (R587R) variant, which has also been reported previously (originally known as SNP7) in Caucasian IBD patients and healthy controls (12), had an allele frequency of more than 10% in both our sarcoidosis patients and the controls. In a case–control association study of the 14429T>G polymorphism, there was no significant difference in allele or genotype frequency between patients and controls (data not shown). The other five mutations (13402C>T, 13543C>T, 13775C>A, 13937G>A, and 14079C>T) are novel. Analysis of *CARD15* exon 4 in the 95 Japanese healthy volunteers showed six variants; four of which are the same as the mutations detected in sarcoidosis. The other two mutations (13927G>A and 14199A>G) are also novel. Table 1 lists a total of 10 *CARD15* variants identified in this study. Based on the results, we then examined the clinical manifestations of the *CARD15* mutations in sarcoidosis patients. The clinical features of the affected individuals are summarized in Table 2. Similar to BS/EOS, only case 7 (onset age: 22 years),

Table 1 *CARD15* variants identified in Japanese patients with sarcoidosis and control individuals

Number	Nucleotide change	Amino acid change	Protein domain	Reported disease	Number of variant alleles	
					Sarcoidosis ($2n = 270$)	Control ($2n = 190$)
1	13402C>T	T245I			1	0
2	13543C>T	A292V	NBD		1	0
3	13599C>T	R311W	NBD	CD, UC	1	3
4	13775C>T	D369E	NBD		1	0
5	13927G>A	R420L	NBD		0	1
6	13937G>A	V423V	NBD		2	1
7	14079C>T	R471C	NBD		6	4
8	14199A>G	T511A	NBD		0	1
9	14429T>G	R587R		CD, UC	36	19
10	14502G>A	A612T		CD, EOS	1	0

CD, Crohn's disease; EOS, early-onset sarcoidosis; NBD, nucleotide-binding domain; UC, ulcerative colitis.

who carried the R471C mutation, had the classic BS/EOS triad of skin, joint, and eye disorders. More recently, in a Spanish cohort with pediatric granulomatous arthritis, a novel *NOD2* (*CARD15*) gene mutation was detected in a patient with an onset age of 18 years (13). Therefore, although it appears that the R471C mutation may be benign, we could not exclude the possibility that the R471C itself has some pathological role or that our case 7 carried other *CARD15* variant(s). Overall, there were no obvious phenotypic features in sarcoidosis patients with these *CARD15* mutations compared with patients without mutations.

CARD15, originally reported as *NOD2*, is a member of the Apaf-1/Ced-4 family of apoptosis regulators and is mainly expressed in monocytes. *CARD15* encodes a protein comprising 2 N-terminal caspase recruitment domains, an NBD, and 10 C-terminal leucine-rich repeats (LRRs) (14). CARD15 is a cytoplasmic protein that serves as an intracellular microbial sensor as it is involved in the recognition of the muramyl dipeptide component of bacterial peptidoglycan, leading to induce immune responses by nuclear factor-κB (NF-κB) activation. *CARD15* was first identified as a susceptibility gene of CD (14, 15), and mutations in this gene also cause BS (8) and EOS (9). However, recent studies have shown that *CARD15* mutations, including disease-causing mutations in CD and BS, are not associated with both familial and nonfamilial sarcoidosis, even in a group of patients with uveitis, in Caucasians (16–19). The exception is the association of the G908R mutation with sarcoidosis in the Greek population (20). In the present study of the Japanese population, we identified 10 variants, including 7 novel missense mutations: 4 in the sarcoidosis patients, 2 in the controls, and 1 in both groups. Of these 10 variants, 2 have previously been reported as disease-associated mutations. It is noteworthy that the *CARD15* mutations R311W and A612T found in European IBD patients were observed in Japanese patients with sarcoidosis. In this study, R311W was detected in 1 of 268 alleles in the sarcoidosis patients and 3 of 190 alleles in the healthy controls, which suggests that the R311W mutation may be associated with resistance to sarcoidosis. Consistent with this conclusion, it was reported that compared with wild-type *CARD15*, EOS/BS-associated *CARD15* mutations are generally located in the NBD and significantly increase basal NF-κB activity, whereas CD-associated *CARD15* variants are within or close to a region with LRRs and generally show normal or reduced levels of

Table 2 Clinical features and *CARD15* mutations in Japanese patients with sarcoidosis

Patient	Age/sex	Age at disease onset	Uveitis	BHL	Lung involvement	Skin lesion	Arthritis	*CARD15* mutations
1	74/F	71	+	−	+	−	−	T245I
2	63/M	61	+	+	−	−	−	A292V
3	51/F	46	+	+	−	−	−	R311W
4	44/F	16	+	+	+	−	−	D369E
5	54/F	55	+	−	−	−	−	R471C
6	48/M	25	+	+	+	−	−	R471C
7	40/M	22	+	+	+	+	+	R471C
8	58/F	57	+	+	−	−	+	R471C
9	69/F	58	+	+	−	−	−	R471C
10	80/M	78	+	+	−	−	−	R471C
11	58/F	58	+	−	−	+	−	A612T

BHL, bilateral hilar lymphadenopathy.

basal activity (21). However, because the functional relevance of genetic variants of NOD proteins in granulomatous inflammatory diseases, such as IBD and sarcoidosis, is still controversial and paradoxical as reported previously (22, 23), further investigation will be needed to understand the precise mechanism by which these variants give rise to susceptibility to such diseases by interaction with other immune mediators, specific microbial components, and other host and environmental factors. The R587R polymorphism (SNP7) observed in this study was also found in European (12) and Korean (24) populations, and a case–control study, which include our cases, showed that the marker exhibited no significant association with CD.

In this study, we showed that *CARD15* mutations are not common even in the Japanese patient population with sarcoidosis. Although the functional significance of these novel *CARD15* mutations is unclear, it is unlikely that these mutations would be involved in the pathogenesis of sarcoidosis in general. However, we could not exclude the possibility that some of these may have some functional contribution. This study and previous studies imply genetic heterogeneity of granulomatous inflammatory disorders. Further genetic analyses of larger or ethnically distinct populations as well as functional studies are required to confirm the effect of *CARD15* variants.

Acknowledgments

We thank Miki Kokubo, Hiroshi Sekiguchi, and Naomi Takahashi for their technical assistance. This work was supported by grants-in-aid from the Ministry of Health, Labor and Welfare of Japan, the Japan Science and Technology Corporation and the Japanese Millennium Project.

References

1. Newman LS, Rose CS, Maier LA. Sarcoidosis. *N Engl J Med* 1997: **336**: 1224–34.
2. Akahoshi M, Ishihara M, Remus N et al. Association between IFNA genotype and the risk of sarcoidosis. *Hum Genet* 2004: **114**: 503–9.
3. Rossman MD, Thompson B, Frederick M et al. HLA-DRB1*1101: a significant risk factor for sarcoidosis in blacks and whites. *Am J Hum Genet* 2003: **73**: 720–35.
4. Valentonyte R, Hampe J, Huse K et al. Sarcoidosis is associated with a truncating splice site mutation in BTNL2. *Nat Genet* 2005: **37**: 357–64.
5. Iannuzzi MC, Rybicki BA, Teirstein AS. Sarcoidosis. *N Engl J Med* 2007: **357**: 2153–65.
6. Shetty AK, Gedalia A. Sarcoidosis: a pediatric perspective. *Clin Pediatr (Phila)* 1998: **37**: 707–17.
7. Tromp G, Kuivaniemi H, Raphael S et al. Genetic linkage of familial granulomatous inflammatory arthritis, skin rash, and uveitis to chromosome 16. *Am J Hum Genet* 1996: **59**: 1097–107.
8. Miceli-Richard C, Lesage S, Rybojad M et al. CARD15 mutations in Blau syndrome. *Nat Genet* 2001: **29**: 19–20.
9. Kanazawa N, Okafuji I, Kambe N et al. Early-onset sarcoidosis and CARD15 mutations with constitutive nuclear factor-kappaB activation: common genetic etiology with Blau syndrome. *Blood* 2005: **105**: 1195–7.
10. Inoue N, Tamura K, Kinouchi Y et al. Lack of common NOD2 variants in Japanese patients with Crohn's disease. *Gastroenterology* 2002: **123**: 86–91.
11. Yamazaki K, Takazoe M, Tanaka T, Kazumori T, Nakamura Y. Absence of mutation in the NOD2/CARD15 gene among 483 Japanese patients with Crohn's disease. *J Hum Genet* 2002: **47**: 469–72.
12. Lesage S, Zouali H, Cezard JP et al. CARD15/NOD2 mutational analysis and genotype-phenotype correlation in 612 patients with inflammatory bowel disease. *Am J Hum Genet* 2002: **70**: 845–57.
13. Arostegui JI, Arnal C, Merino R et al. NOD2 gene-associated pediatric granulomatous arthritis: clinical diversity, novel and recurrent mutations, and evidence of clinical improvement with interleukin-1 blockade in a Spanish cohort. *Arthritis Rheum* 2007: **56**: 3805–13.
14. Ogura Y, Bonen DK, Inohara N et al. A frameshift mutation in NOD2 associated with susceptibility to Crohn's disease. *Nature* 2001: **411**: 603–6.
15. Hugot JP, Chamaillard M, Zouali H et al. Association of NOD2 leucine-rich repeat variants with susceptibility to Crohn's disease. *Nature* 2001: **411**: 599–603.
16. Schurmann M, Valentonyte R, Hampe J, Muller-Quernheim J, Schwinger E, Schreiber S. CARD15 gene mutations in sarcoidosis. *Eur Respir J* 2003: **22**: 748–54.
17. Ho LP, Merlin F, Gaber K, Davies RJ, McMichael AJ, Hugot JP. CARD 15 gene mutations in sarcoidosis. *Thorax* 2005: **60**: 354–5.
18. Martin TM, Doyle TM, Smith JR, Dinulescu D, Rust K, Rosenbaum JT. Uveitis in patients with sarcoidosis is not associated with mutations in NOD2 (CARD15). *Am J Ophthalmol* 2003: **136**: 933–5.
19. Milman N, Nielsen OH, Hviid TV, Fenger K. CARD15 single nucleotide polymorphisms 8, 12 and 13 are not increased in ethnic Danes with sarcoidosis. *Respiration* 2007: **74**: 76–9.
20. Gazouli M, Koundourakis A, Ikonomopoulos J et al. CARD15/NOD2, CD14, and toll-like receptor 4 gene polymorphisms in Greek patients with sarcoidosis. *Sarcoidosis Vasc Diffuse Lung Dis* 2006: **23**: 23–9.
21. Kambe N, Nishikomori R, Kanazawa N. The cytosolic pattern-recognition receptor Nod2 and inflammatory granulomatous disorders. *J Dermatol Sci* 2005: **39**: 71–80.
22. Tanabe T, Ishige I, Suzuki Y et al. Sarcoidosis and NOD1 variation with impaired recognition of intracellular Propionibacterium acnes. *Biochim Biophys Acta* 2006: **1762**: 794–801.
23. Gaya DR, Russell RK, Nimmo ER, Satsangi J. New genes in inflammatory bowel disease: lessons for complex diseases? *Lancet* 2006: **367**: 1271–84.
24. Croucher PJ, Mascheretti S, Hampe J et al. Haplotype structure and association to Crohn's disease of CARD15 mutations in two ethnically divergent populations. *Eur J Hum Genet* 2003: **11**: 6–16.

Tissue Antigens ISSN 0001-2815

Re-evaluation of heterogeneity in HLA-B*510101 associated with Behçet's disease

Y. Takemoto[1]*, T. Naruse[2]*, K. Namba[1], N. Kitaichi[1], M. Ota[3], Y. Shindo[4], N. Mizuki[5], A. Gul[6], W. Madanat[7], H. Chams[8], F. Davatchi[8], H. Inoko[9], S. Ohno[1] & A. Kimura[2]

1 Department of Ophthalmology and Visual Sciences, Hokkaido University Graduate School of Medicine, Sapporo, Japan
2 Department of Molecular Pathogenesis, Medical Research Institute, Tokyo Medical and Dental University, Tokyo, Japan
3 Department of Legal Medicine, Shinshu University School of Medicine, Matsumoto, Japan
4 Department of Ophthalmology, Junon Clinic, Aikawa, Japan
5 Department of Ophthalmology, Yokohama City University School of Medicine, Yokohama, Japan
6 Division of Rheumatology, Department of Internal Medicine, Istanbul University, Istanbul, Turkey
7 Jordan Hospital, Amman, Jordan
8 Rheumatology Research Center, Tehran University for Medical Sciences, Tehran, Iran
9 Department of Molecular Life Science, Basic Medical Science and Molecular Medicine, Tokai University School of Medicine, Isehara, Japan

Key words
Behçet's disease; human leukocyte antigen-B; polymorphism

Correspondence
Akinori Kimura, MD, PhD
Department of Molecular Pathogenesis
Medical Research Institute
Tokyo Medical and Dental University
1-5-45 Yushima
Bunkyo-ku
Tokyo 113-8510
Japan
Tel: +81 3 5803 4905
Fax: +81 3 5803 4907
e-mail: akitis@mri.tmd.ac.jp

Received 11 April 2008; revised 17 June 2008; accepted 8 July 2008

doi: 10.1111/j.1399-0039.2008.01111.x

Abstract

Behçet's disease (BD) is a chronic inflammatory disease characterized by oral aphthous ulcers, genital ulcers, uveitis and skin lesions. Etiology and pathogenesis of BD are not fully elucidated, but the association with human leukocyte antigen (HLA)-B51 or B*5101 has been repeatedly reported. Previous studies have shown that there are few sequence variations in the protein-coding region of B51, while there is a report on many variations in the 5′-flanking region and intron. In this study, HLA-B*5101 gene from 37 individuals including Japanese, Turkish, Jordanian and Iranian patients and healthy controls were fully sequenced to further clarify the B*5101 gene in association with BD. We found that all the patients and healthy controls carried B*510101 with no variation in the 5′-flanking region, exon and intron. However, seven polymorphisms were found in the 3′-flanking region. These polymorphisms composed of six haplotypes that were shared and stretched over the ethnic groups, suggesting that the susceptibility to BD was conferred by the B*510101 itself and not by any genes in linkage disequilibrium with B*510101. In addition, phylogenetic analyses of B*510101 showed that the 3′-flanking sequences followed an evolutional divergence differently from that of the other regions, implying that a unifying selection might operate to conserve B*510101.

Introduction

Human leukocyte antigen (HLA) region that spans about 3.6 Mb and locates on the short arm of chromosome 6 contains a number of multigene families whose products control many functions including the regulation of immune responses and inflammation (1). Most of the genes in the HLA region are polymorphic, especially HLA class I (HLA-A, -B and -C) and class II (HLA-DRB1, -DQA1, -DQB1, -DPA1 and -DPB1); genes show remarkable polymorphisms. The polymorphisms in the HLA genes are concentrated in exon encoding for binding domain of antigenic peptides, and specific alleles of the HLA genes showed strong associations with autoimmune diseases, implying that immune response to certain antigenic peptides might be involved in the pathogenesis. However, strong linkage disequilibria (LD) observed among alleles of genes in the HLA region made it uncertain whether the disease-associated HLA allele itself and/or some HLA-linked genes play a key role in controlling the susceptibility to the disease.

*These authors contributed equally to this work.

Behçet disease (BD) (MIM %109650) is a systemic inflammatory disease characterized by oral aphthous ulcers, genital ulcers, uveitis and skin lesions. BD may also be accompanied by inflammation of other organs, including gastrointestinal, pulmonary and central nervous system (2). Prevalence of BD is higher in a region extending from Middle East to Japan, overlapping with ancient Silk Road (3). The etiology of BD remains unknown, but it is believed both genetic and environmental factors are controlling the susceptibility (4). In 1973, Ohno et al. reported a strong association between BD and serologically defined HL-A5 (5), which was later reclassified to HLA-B5 and then to HLA-B51 and -B52. Following that report, many studies showed that BD was associated with HLA-B51, especially B*5101, in many different ethnic groups, including Japanese (6), Turkish (7), Jordanian (8), Iranian (9), German (7), Spanish (10), Greek (11), Italian populations (12). These observations strongly suggested that HLA-B*5101 itself or a closely linked gene is one of the major risk factors for BD. However, Sano et al. reported that there were at least 24 single nucleotide polymorphisms (SNPs) in the promoter/enhancer region and intron of HLA-B*510101 (previously designated as B*51011) in Japanese population from the analysis of three BD patients and three healthy controls, i.e. the data implied a remarkable heterogeneity of B*510101, at least in Japanese population (13).

In the present study, we determined the genomic sequence of the HLA-B*5101 from BD patients and controls in Japanese, Turkish, Jordanian and Iranian populations to re-evaluate the heterogeneity of B*510101 and to further clarify the association with BD. It was shown that the entire coding region of HLA-B*5101 gene was completely identical among these ethnic groups, but a considerable heterogeneity was observed in the 3′-flanking region forming at least six different B*510101 haplotypes that were found in both the BD patients and the controls at similar frequencies. These observations strongly suggested that there might be a unifying selection pressure on the HLA-B*510101 sequences and that the susceptibility to BD was conferred by the HLA-B*510101 itself and not by any genes in LD with HLA-B*510101.

Materials and methods

Subjects

From a total of 411 individuals (145 BD patients and 266 controls) serologically typed for HLA, 84 patients and 45 controls carrying HLA-B51 were selected. They were genotyped for HLA-B, and 69 patients and 40 controls were found to have HLA-B*5101. From the HLA-B*5101-carrying individuals, 37 individuals, 24 patients with BD (10 Japanese, 3 Turkish, 2 Jordanian and 9 Iranian) and 13 controls (4 Japanese, 3 Turkish, 2 Jordanian and 4 Iranian), were randomly selected and subjected full sequencing of B*5101. Diagnosis of BD was based on the International Study Group Criteria (14). Japanese patients and controls were enrolled at the Junon Clinic, Hokkaido University Hospital, Yokohama City University Hospital and Japan Red Cross Hyogo Blood Center. Iranian, Turkish and Jordanian samples were obtained at the Rheumatology Research Center of Tehran University for Medical Science, the Istanbul University Hospital and the Jordan Hospital, respectively. Blood samples were collected from each individual after informed consent was given. As references, three human B-lymphoblastoid cell lines (B-LCLs) with HLA-B*510101 obtained from 9th and 10th International Histocompatibility Workshop were used; LKT2 (HLA-B*510101/*510101, Japanese origin), LCL721 (HLA-B*510101/*0801, ethnic origin unknown) and BM92 (HLA-B*510101/*510101, Caucasian origin) (15). In addition, 42 individuals with HLA-B51 randomly selected from 364 HLA-genotyped Japanese healthy individuals collected in Tokyo Medical and Dental University were investigated for 3′-flanking sequences of HLA-B gene and for an HLA-linked microsatellite marker, C1_2_5 (16). The study protocol was approved by the ethics committee of the Hokkaido University Graduate School of Medicine, Tokai University School of Medicine and Medical Research Institute, Tokyo Medical and Dental University.

Sequencing of HLA-B gene

Genomic DNA was extracted from peripheral blood leukocytes from HLA-B51-positive individuals by using guanidine thiocyanate or QIAamp DNA Blood Mini Kit (Qiagen, Valencia, CA) and subjected to sequencing-based typing (SBT) of HLA-B gene (15) by using AlleleSEQR HLA kit (Forensic Analytical Molecular Genetics, Chicago, IL). HLA-B genes from DNAs from individuals and B-LCLs carrying HLA-B*5101 were amplified by long-range polymerase chain reaction (PCR) as described previously (16). The PCR products were cloned into a plasmid vector using TOPO XL PCR Cloning Kit (Invitrogen, Carlsbad, CA) and transformed into *Escherichia coli* according to the manufacturer's instructions. Transformants were picked-up and genotyped by the SBT method to select B*5101 clones, and several independent clones were sequenced for the entire PCR region containing the HLA-B gene including promoter/enhance region, exon, intron and 3′ non-flanking region by the primer walking method (17). When at least three independent clones with identical sequences were obtained from each individual heterozygous for B*510101, we confirmed the presence of B*510101. In the case of B*510101 homozygote, at least eight clones were picked-up, and all the clones showed identical sequences. Cycle sequencing reactions were carried out with Big Dye Terminators (ABI, Foster City, CA) version 1.1 sequencing

kits using ABI Prism 3100 DNA Sequencer (ABI). Sequences of 3′-flanking region of the HLA-B gene were determined by PCR-direct sequencing method (17). Nucleotide sequences of B*0702, B*0801, B*5201 and B*5401 reported by Shiina et al. (18) were used as reference in the sequence comparison. Phylogenetic trees of HLA-B alleles were constructed by the unweighted pair-group method using arithmetic average (UPGMA) method using GENETYX software package ver.8 (Genetyx, Tokyo, Japan).

Microsatellite typing

Genotyping of C1_2_5 was performed as described previously (16).

Statistical analyses

Frequencies of alleles in the patients were compared with those in the controls. Relative risk (RR) was calculated to evaluate the strength of association from a 2×2 contingency table, and the statistical significance was evaluated by Fisher exact test. *P* value less than 0.05 was considered to be significant.

Results

As summarized in Table 1, we found that HLA-B*5101 was significantly associated with BD in Japanese, Turkish and Iranian populations with RR ranging from 6 to 10. In Jordanian population, B*510101 gave high RR, but the association was not statistically significant, presumably because of small sample size. To further clarify the association, HLA-B gene was fully sequenced from 37 HLA-B*5101-positive individuals, 24 BD patients and 13 healthy controls, randomly selected from four ethnic groups (Table 1). Three B-LCLs, carrying HLA-B*5101, BM92, LCL721 and LKT2, were also sequenced for the HLA-B gene. Nucleotide sequences of 5′-flanking region (nucleotide position; from −884 to −22), entire exon and intron (nucleotide position; from −21 to 3300) and 3′-flanking region (nucleotide position; from 3301 to 3732) from the samples were determined and compared with those from B*0702, B*0801, B*5201 and B*5401.

To our surprise, there was no sequence variation in the 5′-flanking region and intron of B*510101 among the tested samples including 17 Japanese samples (Table 2). However, there were seven SNPs in the 3′-flanking region, composing of six different B*510101 haplotypes (Figure 1). Five SNPs (at positions of 3449, 3471, 3521, 3525 and 3623) were not specific to B*510101; they can be found in reference HLA-B alleles used in this study, B*0702, B*0801, B*5201 or B*5401 (Table 2). Only two SNPs (at positions of 3586 and 3712) were confined to specific B*510101 haplotypes, haplotype 2 and 4, respectively, although we could not rule out a possibility that these SNPs might be found in non-tested HLA-B alleles.

The distribution of B*510101 haplotypes in BD patients and controls from four ethnic groups are shown in Table 2. Haplotype 2 (H2, Figure 1 and Table 2) was unique to a Turkish patient and a B-LCL BM92 of Caucasian origin, and haplotype 6 (H6) was found only once in the Iranian patients. The other B*510101 haplotypes, H1, H3, H4 and H5 were found in all four ethnic groups (Table 2). The analysis showed that no B*510101 haplotype was specific to BD, suggesting that the susceptibility to BD was controlled by the B*510101 sequence and not by a gene in strong LD with specific B*510101 haplotype(s).

Because most of the SNPs specifying B*510101 haplotypes could be found in other HLA-B alleles, phylogenetic trees were constructed using sequences of 5′-flanking region, exons 2 and 3, other exon, intron and 3′-flanking region to investigate the divergence of B*510101 haplotypes. As shown in Figure 2, phylogenetic trees constructed by the sequences identical to all the B*510101 haplotypes showed similar divergent pattern, albeit the length of tree was relatively long for 5′-flanking sequence and extensively long for exons 2 and 3 (Figure 2A–D). These patterns could

Table 1 Samples tested in this study

Ethnicity	Patient/ control	Number of subjects	B51 carriers, *n* (%)	B*510101 in B51 carriers, *n* (%)	RR by B*510101[a]	Sequenced samples[b]
Japanese	Patient	28	19 (67.9)	19 (100)	10.2 (0.0000002)	10 (2)
	Control	140	24 (17.1)	24 (100)		4 (1)
Turkish	Patient	22	15 (68.2)	11 (73.3)	6.5 (0.001)	3 (2)
	Control	60	8 (13.3)	8 (100)		3 (1)
Jordanian	Patient	35	15 (42.9)	8 (53.3)	3.6 (0.27)	2 (0)
	Control	26	2 (7.7)	2 (100)		2 (0)
Iranian	Patient	60	35 (58.3)	31 (88.6)	6.1 (0.0003)	9 (6)
	Control	40	11 (27.5)	6 (54.5)		4 (0)

RR, relative risk.

[a] RR conferred by B*510101 and *P* value in the parenthesis.

[b] Number of B*510101 homozygotes in parenthesis.

Table 2 HLA-B*510101 haplotypes defined by the polymorphisms in the 3′-flanking region of HLA-B gene identified in this study

	Nucleotide position in the HLA-B gene (bp)							Number of individuals with haplotype								
								Japanese		Turkish		Jordanian		Iranian		
	3449	3471	3521	3525	3586	3623	3712	Patient	Control	Patient	Control	Patient	Control	Patient	Control	B-LCL
B*510101 haplotypes																
H1	T	T	A	T	C	T	C	1	0	0	3	1	0	1	0	LCL721
H2	T	T	T	C	T	T	C	0	0	1	0	0	0	0	0	BM92
H3	T	T	T	C	C	T	C	0	1	2	0	0	1	6	1	
H4	C	C	A	T	C	C	G	11	3	1	0	0	0	3	1	LKT2
H5	C	C	A	T	C	C	C	0	1	1	1	1	1	5	1	
H6	T	T	A	C	C	T	C	0	0	0	0	0	0	0	1	
References																
B*0702	T	T	T	C	C	T	C									PGF
B*0801	T	T	A	T	C	T	C									COX
B*5201	C	C	A	T	C	C	C									AKIBA
B*5401	C	C	A	T	C	C	C									LKT3

B-LCL, B-lymphoblastoid cell line; bp, base pair; HLA, human leukocyte antigen.

be assumed because exons 2 and 3 encoding for antigenic peptide-binding domain, and in part 5′-flanking sequences containing promoter/enhancer, might be under a selective pressure and predate the diversification of human from other higher primates (19, 20). In clear contrast, the 3′-flanking region showed completely different tree pattern (Figure 2E) from those constructed by the other sequences. These observations implied that the SNPs in the 3′-flanking sequences preceded the divergence of B*510101 from B*5201. Alternatively, the 3′-flanking sequence could be divergent before the specification of B*510101, and a unifying selection occurred for the B*510101 coding sequences.

To explore further the evolution of B*510101 haplotypes, B*510101 samples were genotyped for a microsatellite marker C1_2_5. As shown in Table 3, distribution of C1_2_5 alleles in the B*510101 positives was different for each haplotype. Especially, H1, H4 and H5 were significantly associated, i.e. in significant LD, with C1_2_5

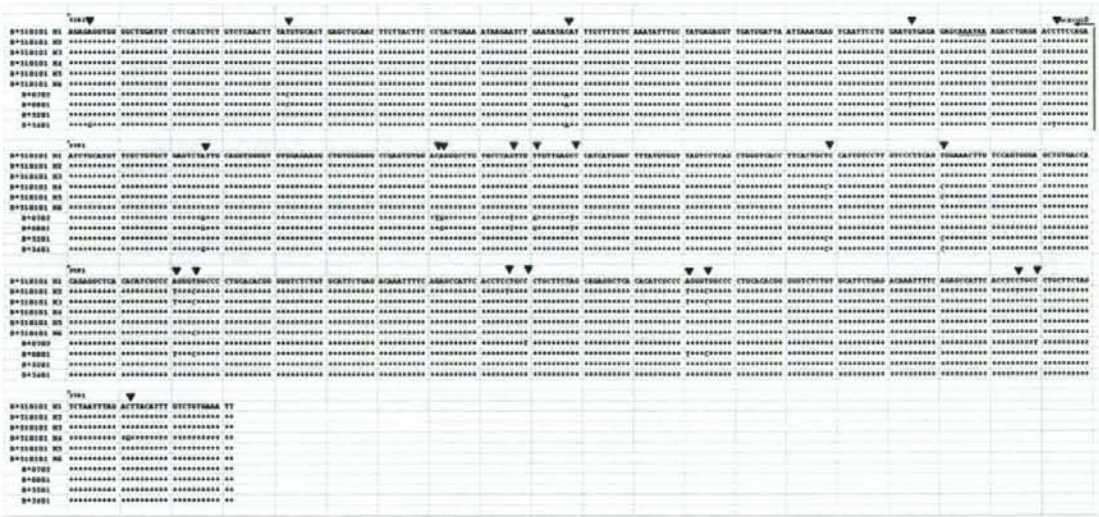

Figure 1 Nucleotide sequences of HLA-B*510101 haplotypes and reference sequences. Full sequences of B*510101 were determined from 37 individuals and classified into six haplotypes by seven polymorphisms in the 3′-flanking region. No sequence variations of B*510101 were found in the 5′-flanking region, exon and intron. A part of exon 8 and 3′-flanking sequences are shown. References were from B*0702, B*0801, B*5201 and B*5401 (18). Polymorphisms found in the 3′-flanking region of HLA-B gene are shown by arrowheads.

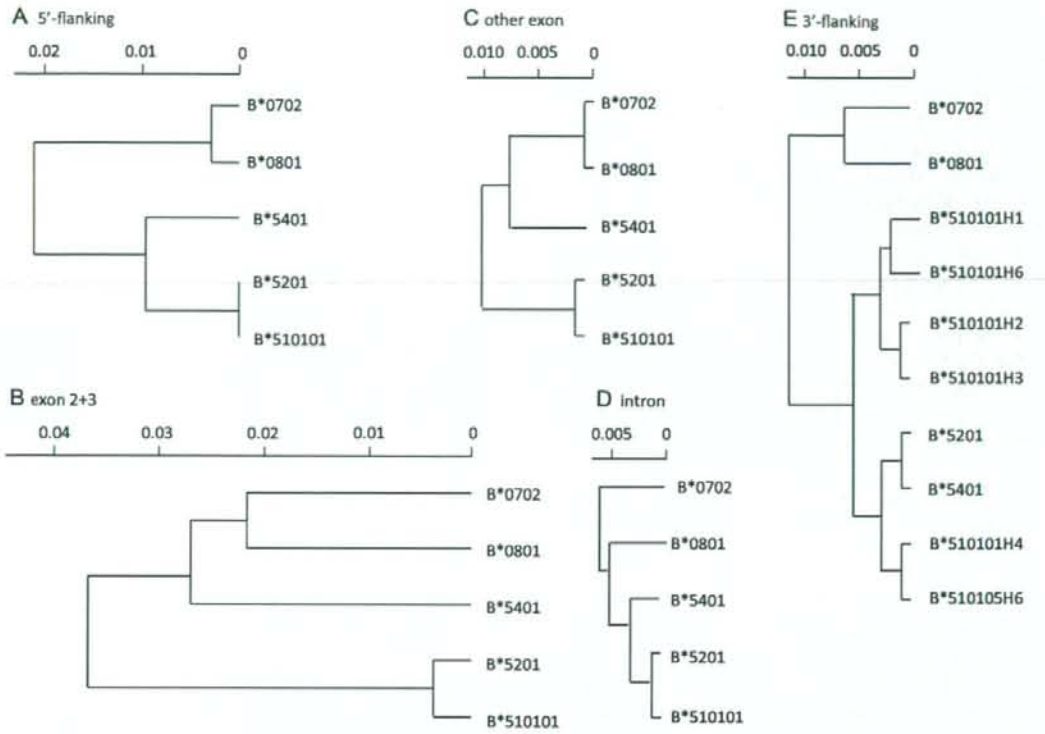

Figure 2 Phylogenetic trees constructed by UPGMA method. Phylogenetic trees were constructed by UPGMA method using 5'-flanking sequence (A), exon 2 and 3 (B), other exon (C), intron (D) and 3'-flanking sequence (E) from B*0702, B*0801, B*5201, B*5401 (18) and B*510101 sequences determined in this study. B*5101010 sequence was identical in 5'-flanking sequence, exon and intron.

alleles 198, 202 and 188, respectively (Table 3). However, C1_2_5 alleles linked to H3 were rather broadly distributed, implying that H3 might be an ancient B*510101. One would argue that B*510101 haplotypes showing strong LD with specific C1_2_5 alleles might be found in specific ethnic groups. However, H1, H3, H4 and H5 were similarly found in all four ethnic groups (Table 2). LD with C1_2_5 alleles was not significant for H2 and H6 because sample size was too small to draw significant conclusion, although LD between H2 and C1_2_5 allele 202 was highly likely (Table 3).

Because two C1_2_5 alleles, 202 and 178, were associated with the susceptibility to BD in Japanese population (21), additional 42 Japanese individuals with HLA-B*5101 were sequenced for the 3'-flanking region of HLA-B gene and genotyped for C1_2_5 to figure out the Japanese B*510101 haplotypes at the population level. The results showed that H1, H4 and H5 were the major B*510101 haplotypes and that the C1_2_5 alleles, 202 and 178, were associated with H4 and H1, respectively, in Japanese population.

Table 3 Distribution of C1_2_5 alleles in the individuals carrying the B*510101 haplotypes

B*510101 haplotypes	*n* (homo)	178	182	188	192	194	196	198	200	202	212	214	Others
H1	6 (1)	0	0	1	0	0	2	6*	0	0	1	1	1
H2	2 (1)	0	0	1	0	0	0	0	0	3	0	0	0
H3	10 (3)	0	2	0	1	1	3	6	2	4	0	0	1
H4	17 (2)	1	0	3	0	0	0	4	3	18**	1	1	3
H5	10 (1)	1	1	9***	0	0	1	2	2	1	1	1	1
H6	1 (0)	0	0	0	1	0	0	1	0	0	0	0	0

Fisher exact *P*: *$P = 0.037$; **$P = 0.012$; ***$P = 0.006$.

Discussion

In the present study, we determined full sequences of HLA-B*5101 from 37 individuals and 3 B-LCLs. We found that all the B*5101 sequences from the tested samples were B*510101 and not B*510102 (22). In addition, B*510101 sequences in this study were identical from −884 to +3448, which include entire HLA-B gene. However, we found seven SNPs in the 3′-flanking region of B*510101, and these SNPs formed six haplotypes.

The most important finding in this study was that the variations found in the 3′-flanking region of B*510101 were observed in the other HLA-B alleles. Because most of the SNPs specifying B*510101 haplotypes could be found in other HLA-B alleles, these SNPs might be preceded by the specification of HLA-B alleles or B*510101 haplotypes were generated from the recombination between an ancestral B*510101 haplotype and other HLA-B alleles in the 3′-flanking region. The latter possibility was unlikely because the SNPs in the 3′-flanking region were not specific to any HLA-B alleles. If the former possibility was true, it was striking that the entire HLA-B*510101 gene, at least for 4332 base pairs from −884 to +3448, was completely conserved among different B*510101 haplotypes. In support of this hypothesis, the phylogenetic tree constructed for the 3′-flanking region was completely different from those constructed for the other regions. This could be explained by a unifying selective pressure operated on the entire HLA-B gene.

Previous studies have suggested that the susceptibility to BD is primarily associated with B*5101, but the previous analyses were limited to the analysis of exon and a part of intron. Our data showed that there was no sequence variation in B*510101, and no specific B*510101 haplotype was associated with BD. This was in good agreement, at least in part, with the observations in previous studies that BD was associated with different C1_2_5 alleles in different ethnic groups, i.e. 178 and 202 in Japanese population (16, 21), 188 in Greek population (21), 188 in Jordanian population (23) and 202 in Italian population (21), because different C1_2_5 alleles were associated with different B*510101 haplotypes that may be predominant in each ethnic group, such as H4 in Japanese population. We found that the C1_2_5 alleles showing strong association with BD in Japanese population, 178 and 202, were in LD with different B*510101 haplotypes, H1 and H4, respectively. These observations strongly suggested that the disease susceptibility was controlled by the B*510101 sequences and not by any polymorphisms in LD with specific B*510101 haplotypes.

Finally, phylogenetic analysis suggested that the entire sequence of B*510101 was conserved. Namely, it could be speculated that the well-conserved structure of the B*510101 might play important roles in immune function and hence in the disease development of BD. This finding is in clear contrast that the sequences around the HLA-B gene showed higher mutation rate than the other regions (18). Further investigations will be required to decipher the potential unifying selective pressure for B*510101 sequences.

Acknowledgments

We are grateful to Drs Takashi Shiina, Jerzy K. Kulski, Daisuke Shichi, Eri F Kikkawa and Yoshihiko Katsuyama for their contributions in the initial course of the study. This study was supported in part by research grants from the Ministry of Health, Labor, and Welfare Japan, the program of Founding Research Centers for Emerging and Reemerging Infection Disease, research grants from the Japan Health Sciences Foundation, a grant-in-aid from the Ministry of Education, Culture, Sports, Science and Technology, Japan and grant-in-aids from the Japan Society for the Promotion of Science.

References

1. Beck S, Trowsdale J. The human major histocompatibility complex: lessons from the DNA sequence. *Annu Rev Genomics Hum Genet* 2000: **1**: 117–37.
2. Sakane T, Takeno M, Suzuki N, Inaba G. Behçet's disease. *N Engl J Med* 1999: **341**: 1284–91.
3. Lewis KA, Graham EM, Stanford MR. Systematic review of ethnic variation in the phenotype of Behcet's disease. *Scand J Rheumatol* 2007: **36**: 1–6.
4. Yazici H, Fresko I, Yurdakul. Behçet's syndrome: disease manifestations, management, and advances in treatment. *Nat Clin Pract Rheumatol* 2007: **3**: 148–55.
5. Ohno S, Aoki K, Sugiura S, Nakayama E, Itakura K, Aizawa M. HL-A5 and Behçet's disease. *Lancet* 1973: **7842**: 1383–4.
6. Mizuki N, Ota M, Katsuyama Y et al. HLA-B*51 allele analysis by the PCR-SBT method and a strong association of HLA-B*5101 with Japanese patients with Behçet's disease. *Tissue Antigens* 2001: **58**: 181–4.
7. Kötter I, Günaydin I, Stübiger N et al. Comparative analysis of association of HLA-B*51 suballeles with Behçet's disease in patients of German and Turkish origin. *Tissue Antigens* 2001: **58**: 166–70.
8. Verity DH, Wallace GR, Vaughan RW et al. HLA and tumor necrosis factor (TNF) polymorphisms in ocular Behçet's disease. *Tissue Antigens* 1999: **54**: 264–72.
9. Mizuki N, Ota M, Katsuyama Y et al. HLA class I genotyping including HLA-B*51 allele typing in the Iranian patients with Behçet's disease. *Tissue Antigens* 2001: **57**: 457–62.
10. Gonzalez-Escribano MF, Rodriguez MR, Walter K, Sanchez-Roman J, Garcia-Lozano JR, Nunez-Roldan A. Association of HLA-B51 subtypes and Behçet's disease in Spain. *Tissue Antigens* 1998: **52**: 78–80.
11. Koumantaki Y, Stavropoulos C, Spyropoulou M et al. HLA-B*5101 in Greek patients with Behçet's disease. *Hum Immunol* 1998: **59**: 250–5.

12. Kera J, Mizuki N, Ota M et al. Significant associations of HLA-B*5101 and B*5108, and lack of association of class II alleles with Behçet's disease in Italian patients. *Tissue Antigens* 1999: **54**: 565–71.
13. Sano K, Yabuki K, Imagawa Y et al. The absence of disease-specific polymorphisms within the HLA-B51 gene that is the susceptible locus for Behçet's disease. *Tissue Antigens* 2001: **58**: 77–82.
14. International Study Group for Behçet's Disease. Criteria for diagnosis of Behçet's disease. *Lancet* 1990: **335**: 1078–80.
15. Adams SD, Barracchini KC, Simonis TB, Stroneck D, Marincola FM. High throughput HLA sequence-based typing (SBT) utilizing the ABI Prism 3700 DNA Analyzer. *Tumori* 2001: **87**: S40–3.
16. Ota M, Mizuki N, Katsuyama Y et al. The critical region for Behçet disease in the human major histocompatibility complex is reduced to a 46-kb segment centromeric of HLA-B, by association analysis using refined microsatellite mapping. *Am J Hum Genet* 1999: **64**: 1406–10.
17. Matsuzawa Y, Sano K, Shiina T et al. Development of a novel method for genome sequencing of the entire HLA-B gene. In: Hansen HA, ed. *Immunobiology of the Human MHC*, Vol. II. *Seattle: Seattle 2006 IHWG Press, 2006, 89–92.*
18. Shiina T, Ota M, Shimizu S et al. Rapid evolution of major histocompatibility complex class I genes in primates generates new disease alleles in humans via hitchhiking diversity. *Genetics* 2006: **173**: 1555–70.
19. Hughes AL, Yeager M. Natural selection at major histocompatibility complex loci of vertebrates. *Annu Rev Genet* 1998: **32**: 415–35.
20. Klein J, Satta Y, O'hUigin C, Takahata N. The molecular descent of the major histocompatibility complex. *Annu Rev Immunol* 1993: **11**: 269–95.
21. Mizuki N, Ota M, Yabuki K et al. Localization of the pathogenic gene of Behçet disease by microsatellite analysis of three different populations. *Invest Ophthalmol Vis Sci* 2000: **41**: 3702–8.
22. Cox ST, McWhinnie AJ, Robinson J et al. Cloning and sequencing full-length HLA-B and -C genes. *Tissue Antigens* 2003: **61**: 20–48.
23. Mizuki N, Yabuki K, Ota M et al. Microsatellite mapping of a susceptible locus within the HLA region for Behçet's disease using Jordanian patients. *Hum Immunol* 2001: **62**: 186–90.

Eye (2009) 23, 222–229

www.nature.com/eye

LABORATORY STUDY

New susceptibility locus for high myopia is linked to the uromodulin-like 1 (*UMODL1*) gene region on chromosome 21q22.3

R Nishizaki[1,2], M Ota[3], H Inoko[4], A Meguro[1], T Shiota[3], E Okada[2], J Mok[4,5], A Oka[4], S Ohno[6] and N Mizuki[1]

[1]Department of Ophthalmology, Yokohama City University School of Medicine, Kanagawa, Japan

[2]Okada Eye Clinic, Kanagawa, Japan

[3]Department of Legal Medicine, Shinshu University School of Medicine, Nagano, Japan

[4]Department of Basic Medical Science and Molecular Medicine, Tokai University School of Medicine, Kanagawa, Japan

[5]Laboratory of Ophthalmology and Visual Science, Catholic Research Institutes of Medical Science College of Medicine, The Catholic University of Korea, Seoul, Korea

[6]Department of Ophthalmology, Hokkaido University School of Medicine, Hokkaido, Japan

Correspondence: M Ota, Department of Legal Medicine, Shinshu University School of Medicine, 3-1-1 Asahi Matusmoto, 390-8621 Japan. Tel: +81263373217; Fax: +81263373084; E-mail: otamasao@sch.md.shinshu-u.ac.jp

Received: 12 November 2007
Accepted in revised form: 15 April 2008
Published online: 6 June 2008

Abstract

Purpose **To ascertain and define the position of a potential disease susceptibility gene around *D21S0083i* prioritized during our previous whole genome case-control association analysis with 27158 microsatellite markers, in Japanese high-myopia patients.**
Methods **520 high myopic patients and 520 healthy controls were genotyped using 39 SNPs distributed around *D21S0083i* on chromosome 21q22.3.**
Results **Only 1 SNP (rs2839471) of 39 SNPs was significant after correction for multiple testing (allele T: $P = 0.00027$, $Pc = 0.01$, $OR = 1.684$). The SNP (rs2839471) did not reside in haplotype blocks constructed by the pair-wise linkage disequilibrium between the SNPs.**
Conclusions **The SNP (rs2839471) is suggested to be located in the frequent recombinant region within *UMODL1*. Together this region might play a critical role for susceptibility to high myopia, and warrants further confirming studies and investigations as to the mechanisms by which *UMODL1* may contribute to myopia.**
Eye (2009) **23,** 222–229; doi:10.1038/eye.2008.152; published online 6 June 2008

Keywords: high myopia; susceptibility; *UMODL1*

Introduction

Myopia, diagnosed as a spherical refractive error of −0.50 D or below, is the most common eye disorder in the modern world. High myopia (≤−6.00D) is associated with the increased risk of several ocular diseases, such as glaucoma, retinal detachment, visual impairment, and blindness.[1,2]

In a population of Japanese students three to 17 years old, the prevalence of myopia increased from 49.3 to 65.6%.[3] In other countries, the prevalence of myopia shows variable ratio (36.7–87.2% in a Chinese, 19.8–62.1% in a general Asian group, 5.2–40.5% in a Caucasian group aged 5–17 years, and 2.3–14.7% in Australian children aged 4–12 years).[4–7] These phenomena indicate a similar trend that the incidence of myopia is increasing from an early age in the general populations. Prevalence rates among different countries show considerable variability, but confirm that myopia affects a significant proportion of the population in many countries.

Myopia is a complex disease reflecting multiple interactions between genetic and environmental factors, and the aetiology of myopia has yet to be conclusively elucidated. However, several epidemiological studies have shown that several environmental factors, such as proximity to work, higher educational background, occupation, urban region, and socioeconomic status are important risk factors for myopia.[8–14]

On the other hand, determining the role of genetic factors in the development of nonsyndromic myopia has been hampered by the high prevalence, genetic heterogeneity, and clinical spectrum of this condition. Twin studies estimate a notable heritability value more than 0.5–0.87, indicating the proportion of the total phenotypic variance of genes. Furthermore, the importance of genetic factors in ocular

refraction has been implicated by the high heritability and strong familial effects observed in the previous twin studies, as well as parental and sibling studies.[15–18] Moreover, susceptibility genes for myopia have been recently identified in 14 genomic loci (MYP1 on Xq28, MYP2 on 18p, MYP3 on 12q, MYP4 on 7q, MYP5 on 17q, MYP6 on 22q12, MYP7 on 11p13, MYP8 on 3q26, MYP9 on 4q12, MYP10 on 8p23, MYP11 on 4q22-q27, MYP12 on 2q37.1, MYP13 on Xq23-q25, and MYP14 on 1p36).[17,19–27] Although several of the loci have not been replicated by experimental evidence as myopia and high-myopia candidate loci (MYP6-14), one study suggested the potential association of the MYP3 locus with autosomal dominant high myopia in approximately 25% of 51 UK families.[28] The polymorphisms of the transforming growth β-induced factor (*TGIF*) gene within the MYP2 locus were not associated with the high-myopia phenotype.[29,30]

Recently, we performed a whole-genome case–control association analysis of high myopia using 27 158 microsatellite markers and ultimately found significant association of 147 markers with high myopia (manuscript submitted). One of the 147 positive markers was located on chromosome 21q22.3 (microsatellite marker *D21S0083i*). Here, we dissected the position of the candidate susceptibility gene by SNP genotyping around the novel candidate region (*D21S0083i*).

Materials and methods

Subjects

A total of 520 high myopic individuals of Japanese ethnicity with a spherical equivalent of less than −9.25 D at least in one eye and an abnormal axial elongation were recruited from the Okada Eye Clinic and Yokohama City University. Equal numbers of individuals of Japanese origin with normal vision were recruited from Tokai University as a control population group. The average (± SD) age in the high myopic group was 39.7 ± 12.07 years (range: 3–77 years) and the male/female ratio was 1.0:1.3. The average age of the control group was 41.2 ± 11.67 years (range: 25–75 years), and the male/female ratio was similar (1.0:1.2).

The high myopic participants underwent a non-cycloplegic refraction test with an autokerato-refractometer (ARK-700K; NIDEK, Aichi, Japan/KR-8100P; Topcon, Tokyo, Japan). The patients had no known ocular disorders that could predispose them to high myopia, such as glaucoma, keratoconus, posterior staphyloma, or Marfan syndrome. The axial lengths of all affected subjects were measured with a pachymeter (AL-2000; TOMEY, Aichi, Japan). The average of axial length in the high myopic group was 27.8 ± 1.27 mm (range: 20.3–33.1 mm) for the right eye and 27.8 ± 1.29 mm (range: 23.9–34.7 mm) for the left eye; in this group, the average keratometric value was 43.9 ± 1.56 D (range: 39.5–50.3 D) for the right eye and 43.9 ± 1.58 D (range: 39.–53.0 D) for the left eye. This study protocol adhered to the tenets of the Declaration of Helsinki.

These subjects are same cohort used in our previous whole-genome case–control association study.

SNP genotyping

We selected one locus located on chromosome 21q22.3 (microsatellite marker *D21S0083i*) potentially associated with high myopia. The SNPs distributed around this candidate microsatellite marker were selected from the dbSNP database at the NCBI homepage (build 35), UCSC Genome Browser webpage, JSNP database,[31] and the SNP database of Applied Biosystems. The SNPs were selected for analysis based on the following criteria: (a) location within the 200 kb region around the candidate microsatellite marker (100 kb on either side); (b) >10% minor allele frequency (MAF) in the Japanese population; (c) >0.3 average heterozygosity; (d) marker density of at least one SNP per 5 kb; and (e) availability for validated assays. A total of 39 SNPs were selected for calculation of significant difference, linkage disequilibrium (LD), and haplotype analysis.

The SNP genotyping was performed using TaqMan® SNP Genotyping Assays, according to manufacturer's instructions. Reactions were performed with the ABI GeneAmp® PCR System 9700 thermal cycler, and the ABI PRISM® 7900HT Sequence Detection System (Applied Biosystems, Foster City, CA, USA), using a 384-well block module for measuring fluorescence. The SDS software version 2.0 was used for allelic discrimination analysis (Applied Biosystems). Two nanograms of genomic DNA were used as template in the PCR amplification reactions.

Statistical analysis

To estimate statistical significance of comparisons between the high-myopic and control populations, we used the χ^2 test and Fisher's exact test for 2 by 2 and 2 by m contingency tables for SNPs and haplotypes (GDBS: Genome Diversity Database System; http://www.jbirc.aist.go.jp/gdbs/index.html). For genotype frequency analysis, we employed the exact test, which was implemented using the Markov chain Monte Carlo simulation method for 2 by m contingency tables. We defined a P-value of less than 0.05 as statistically significant for all statistical analyses. The statistically

significant *P*-value was corrected by Bonferroni's correction (P_c).

The pairwise relationship in SNPs or haplotypes was estimated by odds ratio (OR) and 95% confidence intervals (CIs) using the JavaStat Webpage. The SNPs genotyping in the control population was analysed for deviation of genotype frequencies from the Hardy–Weinberg equilibrium (HWE) using the procedure from the GDBS web page. The LD patterns, haplotype block structure, and haplotype frequency analysis for all SNPs with MAF >10% in both populations were identified using the block definition of Gabriel *et al*, and was based on 95% CI of D' with implementation of Haploview ver3.32 software.[32,33] LocusView was used to obtain generated images of candidate regions annotated with the haplotype analysis results.

Results

Our previous study reporting a genome-wide association analysis with 27 158 microsatellite markers identified 21 markers as new candidate loci for high myopia (manuscript submitted). We characterized the novel candidate region around one microsatellite marker (*D21S0083i*; $[AC]_n$; allele 4 in 15 alleles; Fisher's $P = 0.016$, OR = 1.34), and performed an association analysis using 39 SNPs and 10 constructed haplotypes located on chromosome 21q22.3 (Figure 1). The SNPs were principally located within four possible candidate genes: zinc-finger protein 295 (*ZNF295*, position: 42280009-42303519), chromosome 21 open reading frame 121 (*C21orf121*, position: 42315261-42318129), chromosome 21 open reading frame 128 (*C21orf128*, position: 42395313-42401627), and uromodulin-like 1 (*UMODL1*, position: 42356137-42436174). The allelic and genotype frequencies of 39 SNPs in the case and control groups are listed in Table 1. The SNP (rs220271: SNP A17) near the *D21S0083i* microsatellite showed a significant association with high myopia ($P = 0.028$, OR = 1.219, 95% CI: 1.026–1.449). Two SNPs (rs2839430 and rs1628526; SNP A2 and A6) in the *ZNF295* gene and four SNPs (rs220271, rs220143, rs220148, and rs2839471; SNP A17, A25, A26, and A32) in the *UMODL1* and *C21orf128* genes showed statistical significance. Allele T-positive (rs 2839471; A32) phenotype was strongly associated with disease susceptibility ($P = 0.00027$, $P_c = 0.01$, OR = 1.684). The alleles of two SNPs (rs915837 and rs150796: SNP A4 and A12) differed significantly from the expected Hardy–Weinberg values (probability test) in the control populations ($P < 0.05$), therefore, these SNPs were excluded from the haplotype analysis. All SNPs, except SNP A32 (rs2839471), preliminarily showing statistical significance were later confirmed as not significant after Bonferroni's correction. The haplotype block structure was analysed using SNPs with MAF>10%, and 10 haplotype blocks were found. Two haplotype blocks showed statistical significance between cases and controls: Block 1, GAG (SNP A3-A5-A6, $P = 0.0493$, OR = 1.189, 95% CI: 1.000–1.414), including *ZNF295*, and Block 6, ACG (SNP A25-A26-A27, $P = 0.0394$, OR = 1.228, 95% CI: 1.010–1.494), including *UMODL1* and *C21orf128* (Table 2, Figure 1). However, their significance disappeared after correction for multiple testing.

Discussion

The aim of this study was to search for a candidate gene for high myopia around the microsatellite marker *D21S0083i*, which showed statistically significant association with high myopia by a previous genome-wide pooled DNA association mapping study (manuscript submitted). We used 39 SNPs located on chromosome 21q22.3 around the microsatellite marker (*D21S0083i*) to define critical regions influencing disease susceptibility.

Several SNPs within the *ZNF295*, *UMODL1*, and *C21orf128* genes showed statistically significant association with high myopia. The SNP rs2839430 (SNP A2) located in the 3′-UTR region of *ZNF295* showed a statistically strong association ($P = 0.008$) with high myopia, although the MAF was low. As the sequence and structural motifs of the 3′-UTR often influence mRNA stability,[34] the SNP A2 may play a critical role in the regulatory process of *ZNF295* gene expression levels. The *ZNF295* gene, spanning approximately 24 kb, consists of five exons and encodes two protein isoforms: ZNF295L and ZNF295S. The ZNF295 protein belongs to the family of Pokemon (POK) proteins and contains a BTB (POZ) domain at its N-terminus and C2H2-type zinc-finger domain at its C-terminus. The ZNF295, ubiquitously expressed in human foetal and adult tissues, acts as a repressor of transcriptional activity and a cofactor of another POK protein ZFP161, being involved in the ZFP161-regulated pathway such as dopaminergic neurotransmission.[35]

The vast majority of individuals with high myopia are characterized by an increase in ocular axial length and scleral thinning. Although the exact mechanism underlying this axial length elongation has yet to be defined, it is presumed that a blurred image or light projected onto the retina induces the secretion of some substance from cells such as the visual, amacrine, horizontal, and bipolar cells, which evokes transfer of the signal to the sclera, thus leading to scleral remodelling and axial elongation. Stone *et al*[36] reported that retinal dopamine and its metabolite reduces form-deprivation myopia with axial length elongation in the chick model.

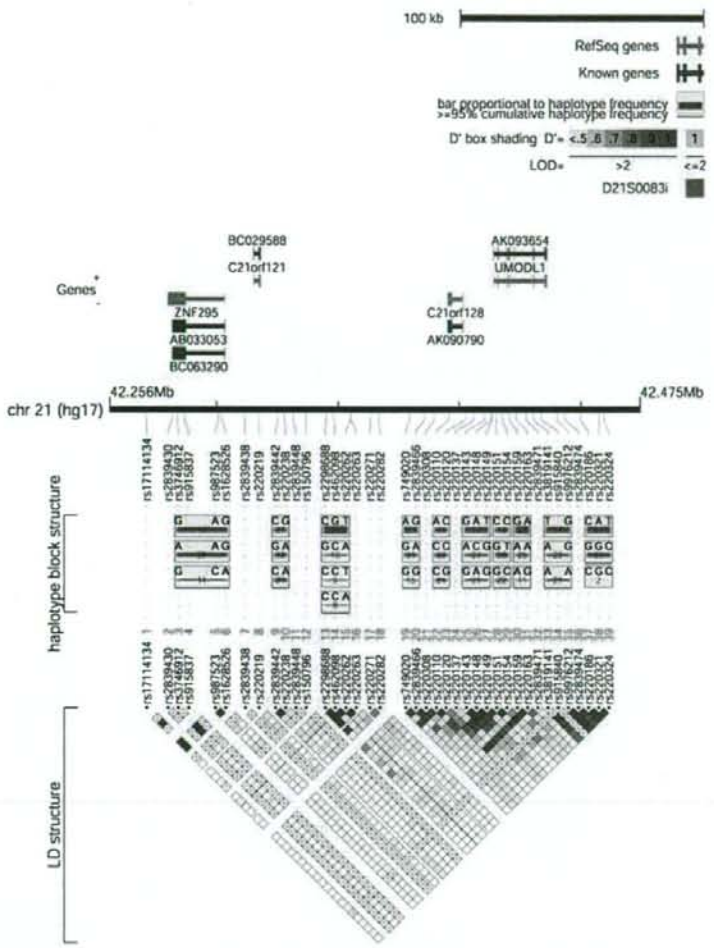

Figure 1 Structures of LD and haplotype block from rs17114134 to rs220324 on chromosome 21q22.3. Pairwise LD between SNPs, as measured by *D'* in high-myopia patients and control individuals. Location of genes and the 39 SNPs are shown throughout the 219 Kb length lying D21S0083i on 21p22.3. Ten haplotype blocks are constructed by high LD between SNPs.

Deviation of this bidirectional interaction between *ZNF295* and *ZFP161* regulation might induce myopization following ocular axial elongation. In contrast, a mutation screening study by Scavello *et al*[37] reported that *ZFP161* was not associated with the myopia phenotypes.

The *UMODL1* gene spans approximately 80 kb, consists of 23 exons and encodes two major transcripts generated by alternative splicing. The two proteins, UMODL1L and UMODL1S, contain multiple domains typically found in extracellular matrix proteins, including an EMI (emilin) domain, WAP (whey acidic protein) domain, EGF_CA (calcium-binding EGF-like) domain, FN3 (fibronectin type 3) domain, SEA (sea urchin sperm protein, enterokinase, agrin) domain, ZP (zona pellucida) domain, and TRANS (transmembrane) domain. Altogether, this suggests that UMODL1 proteins may be secreted and associated with extracellular matrix proteins involved in cell-to-cell and cell-to-extracellular matrix adhesion and in cell migration.[38,39] Consistent with this, results from a linkage study identified significant linkage for familial high myopia on chromosome 12q21–23, a region, which includes extracellular matrix genes such as *lumican*, *decorin*, and *DSPG3* (dermatan sulphate proteoglycan-3).[21] The synthesis and degradation of the extracellular matrix may influence the maintenance of scleral elasticity, strength, and thickness.[40]